

Near Earth Asteroid Scout Thrust and Torque Model

Andrew Heaton¹ and Naeem Ahmad²
NASA Marshall Space Flight Center, Huntsville, AL 35812

Kyle Miller³
Embry-Riddle Aeronautical University, Prescott, AZ 86301

The Near Earth Asteroid (NEA) Scout is a solar sail mission whose objective is to scout at least one Near Earth Asteroid in preparation for manned missions to asteroids. NEA Scout will use a solar sail as the primary means of propulsion. Thus it is important for mission planning to accurately characterize the thrust of the sail. Additionally, the solar sail creates a relatively large solar disturbance torque that must be mitigated. For early mission design studies a flat plate model of the solar sail with a fixed center of pressure was adequate, but as mission concepts and the sail design matured, greater fidelity was required. Here we discuss the progress to a three-dimensional sail model that includes the effects of tension and thermal deformation that has been derived from a large structural Finite Element Model (FEM) developed by the Langley Research Center. We have found that the deformed sail membrane affects torque relatively much more than thrust. We have also found that other than uncertainty over the precise shape, the effect of small (~ millimeter scale) wrinkles on the diffusivity of the sail is the leading remaining source of uncertainty. We demonstrate that millimeter-scale wrinkles can be modeled analytically as a change in the fraction of specular reflection. Finally we discuss the implications of these results for the NEA Scout mission.

Nomenclature

| | | |
|-------------|---|--|
| SLS | = | Space Launch System |
| F_t | = | tangential force [N] |
| F_n | = | normal force [N] |
| A | = | sail area [m ²] |
| P | = | pressure (N/m ²) |
| \tilde{r} | = | total reflectivity |
| s | = | specular reflectivity fraction |
| α | = | solar incidence angle [degrees] |
| B_f | = | front side non-Lambertian coefficient |
| B_b | = | back side non-Lambertian coefficient |
| e_f | = | front side emissivity |
| e_b | = | back side emissivity |
| BRDF | = | Bi-directional Reflectance Distribution Function |
| AOI | = | Angle Of Incidence [degrees] |
| AAD | = | Average Angle of Deviation [degrees] |
| MAD | = | Maximum Angle of Deviation [degrees] |
| FEM | = | Finite Element Model |
| GSM | = | Generalized Sail Model |
| AMT | = | Active Mass Translator |

¹ Senior Aerospace Engineer, EV42/ Guidance, Navigation and Mission Analysis Branch, NASA Marshall Space Flight Center.

² Aerospace Engineer, EV42/ Guidance, Navigation and Mission Analysis Branch, NASA Marshall Space Flight Center.

³ Spring 2016 Intern, / Guidance, Navigation and Mission Analysis Branch, NASA Marshall Space Flight Center.

I. Introduction

NEA Scout will launch as a secondary payload on the first SLS-Orion mission. NEA Scout will perform a small trim maneuver shortly after deploy from the spent SLS upper stage using a cold gas propulsion system, but from that point on will depend entirely on the solar sail for thrust. As such, it is important to accurately characterize the thrust of the sail in order to achieve mission success. Additionally, the solar sail creates a relatively large solar disturbance torque that must be mitigated. For early mission design studies a flat plate model of the solar sail with a fixed center of pressure was adequate, but as mission concepts and the sail design matured, greater fidelity was required. Also as the NEA Scout project proceeded, the original quadrant sail design failed to meet mission requirements due to thermal buckling of the thin metal booms, which originally were not shielded from the sun. The design was successfully changed to a single sail from a four-quadrant sail, allowing the booms to be permanently shielded from the sun for the duration of the mission, thus preventing the predicted boom buckling and leading to disturbance torque predictions smaller by 2-3 orders of magnitude. Additionally optical testing that built upon the results of earlier tests predicts an increase in the effective diffusivity of the sail material due to millimeter-scale wrinkling. Finally, many off-nominal sail models that allow for greater shape distortion and thus disturbance torques have been analyzed, and some have been modeled in the full sail control simulation. Here we discuss the above results and their implications for the NEA Scout mission.

II. Sail Optical Model

The sail material for NEA Scout consists of a thin (2.5 micrometer) CP1 polymer coated with 10 nanometers of aluminum on the front side and an uncoated back side. Thus the optical properties of the sail are essentially those of Aluminum. The optical model for the sail dates back to a model originally derived in 1978 for the Halley Comet Rendezvous project at JPL [2]. This optical model was later reproduced in Wright and McInnes and appears in Equations (1) and (2).

$$F_t = -PA(1 - \tilde{\mathbf{r}}\mathbf{s}) \cos(\alpha) \sin(\alpha) \quad (1)$$

$$F_n = -PA(1 + \tilde{\mathbf{r}}\mathbf{s}) \cos^2(\alpha) - PAB_f(1 - \mathbf{s})\tilde{\mathbf{r}} \cos(\alpha) - PA(1 - \tilde{\mathbf{r}})\left(\frac{e_f B_f - e_b B_b}{e_f + e_b}\right) \cos(\alpha) \quad (2)$$

The terms of equations (1) and (2) are defined in the nomenclature. The equations are derived in the body reference frame of the solar sail. Equation (1) is the tangential force, or force in the plane of the sail, while Equation (2) describes the normal force, or force orthogonal to the plane of the sail. A perfectly flat solar sail is assumed in the derivation of these equations.

In 1978 JPL also derived what essentially became standard values for the coefficients in Equations (1) and (2) and they have been used by NASA since then in many preliminary mission studies. In 2015, we published an extensive review and update to these coefficients. [3] The 1978 coefficients appear in Table 1 and the updated coefficients appear in Table 2. Note that the coefficients published by JPL in 1978 were derived for material that had chromium

on the back side of the sail for thermal reasons, while the updated coefficients do not. Thus the emissivities are quite different.

| Coefficient | \tilde{r} | s | B _f | B _b | e _f | e _b |
|-------------|-------------|------|----------------|----------------|----------------|----------------|
| Value | 0.88 | 0.94 | 0.79 | 0.55 | 0.05 | 0.55 |

Table 1) Sail thrust model optical coefficients from Halley’s Comet Solar Sail mission tests [3, 4]

| Coefficient | \tilde{r} | s | B _f | B _b | e _f | e _b |
|-------------|-------------|---------|----------------|----------------|----------------|----------------|
| Value | 0.91 | 0.94 | 0.79 | 0.67 | 0.025 | 0.27 |
| | +/-0.005 | +/-0.04 | +/-0.05 | +/-0.05 | +/-0.005 | +/-0.005 |

Table 2) Updated optical coefficients based on review of historical test data (various pre-2007 tests)

The coefficients for total reflectivity and the emissivities have been tested rather precisely and the uncertainty associated with them is small. However the three coefficients associated with diffusivity (fraction of specular reflection, and the front and back non-Lambertian coefficients) have a greater uncertainty associated with them. A large part of the uncertainty is lack of sufficient test data for diffusivity. Diffusivity tests are generally accomplished by a Bi-directional Reflectance Distribution Test (BRDF), which requires a more complicated test than a simple reflectance test. Although diffusivity has been measured less often, there are sufficient tests to establish a baseline for pristine material, and the number appearing for specular fraction of reflection in Table 1 is reasonable for pristine (unwrinkled) material. However a much more limited set of tests on wrinkled material strongly suggested that millimeter-scale wrinkles can lead to an effective increase in diffusivity. Based on these results, NASA conducted additional optical testing in late 2015 and the results of these tests were analyzed in early 2016.

III. Optical Testing Analysis and Results

The test set up for the NEA Scout optical test is depicted in Figure 1. The optical test was conducted by Bill Witherow of MSFC [ref]. The purpose of the test was to measure light returned from 10² cm areas of the sail in order to capture the effects of wrinkles on diffuse reflection. A classic BRDF will measure diffusivity of the material at the microscopic scale only. Since the sail must be folded and packed, it will be extremely wrinkled upon deployment, so the effect of wrinkles on global sail optical properties must be assessed. There are different scales to the wrinkles. Those large enough to be approximately on the scale of a meter to centimeters are considered “macroscale”, and can be modeled in structural Finite Element Models (FEMs) at a relatively high level of detail. Wrinkles on the scale of millimeters to 10s of micrometers are considered “mesoscale” and cannot easily or accurately be modeled by a FEM or other relatively high level modeling technique. This is the scale of interest to NEA Scout. Wrinkles smaller than 10s of micrometers are generally considered as a material roughness that can affect optical properties, and thus those

effects are captured by the classic BRDF test for diffusivity. Wrinkles at the micrometer scale (we which call “microscale”) also are not affected much if at all by folding and packing.

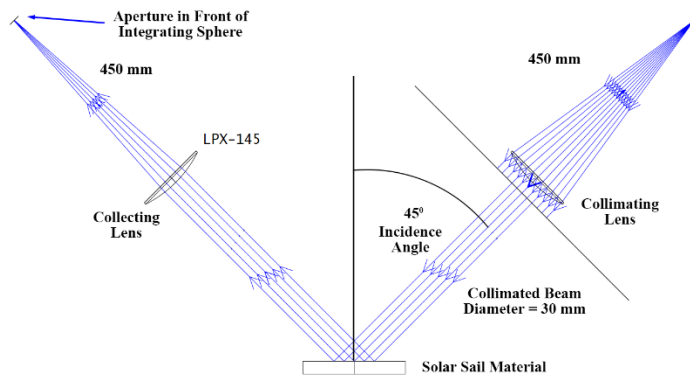


Figure 1) Reflectance Test Optical Setup

In Figure 2 are square areas 10 cm² in size of the 2.5 micrometer thick CP1 sail material. Within the square areas are circular lighted areas which are caused by a laser beam that has been collimated as in Figure 1. Each laser image on the test material was measured at a different time and collected into the single picture shown in Figure 2. This figure demonstrates how light was collected over ~ 10 cm² areas of the sail with a circular beam pattern. The light was focused in areas roughly the size of the lighted circles in Figure 1, and this light was captured at return incidence angles of 2,4,6,8, 10 and 12 degrees, to provide data for an “areal BRDF” analysis.

Several caveats for this test should be discussed. One is the presence of (relatively) large wrinkles in the corners of the material where it is affixed to the supporting structure. These large wrinkles dominate that portion of the test material and comparative analysis of the optical test results show they had a significant effect on the results. These wrinkles can be considered macroscale effects, and while such features are possible or even likely on a solar sail deployed in space, the macroscale wrinkles in Figure 2 are strongly affected by gravity and cannot be considered completely realistic. Also macroscale wrinkles on a solar sail in space will likely be confined to a relatively small portion of the sail. Thus we excluded results from areas around the corners. Another caveat is that the sail material used was not manufactured to flight standards, and so the Aluminum coating was either insufficiently thick or unevenly distributed such as to allow a fairly high amount of transmission. Thus the results had to be normalized to account for transmission. Another caveat is that the laser power varied quite a bit over the course of each test (up to 6 %), so that the results were fairly noisy. The final caveat has to do with the quality of the reflection, as can be seen in in Figure 3. Here the images captured are provided by placing white optical material in front of the reflected light coming off of the sail material that captures the light after it is reflected.

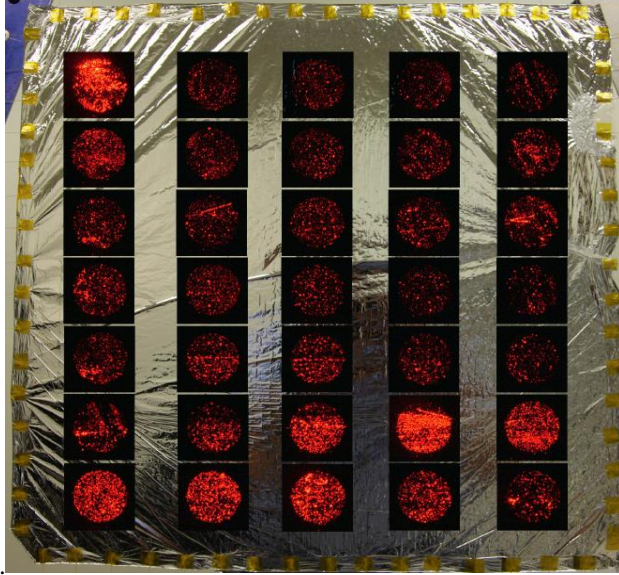


Figure 2) Test Material Showing Size of Illuminated Test Areas

Note that the light is distorted when compared with the images in Figure 2, which were created by backlighting the material with a laser powerful enough to penetrate the material (which as discussed above was transmissive above what is desirable for flight material). Some of the distortions in Figure 3 likely were caused by either test article dynamics by simple misalignment of the material from test to test. Due to all the above effects (macroscale wrinkles, transmission, laser variability, dynamics, and misalignment), the test data had a wide variance and low precision, and so we carefully selected only what we considered the highest quality results from the various sectors in Figure 2. Specifically, we were able to eliminate certain test regions which were affected by macroscale wrinkles and dynamic movements of the test stand that degraded the results appreciably. We thus qualitatively screened about half of the test regions shown in Figures 2 and 3.



Figure 3) Test Material Showing Shape of Reflected Light Pattern with Grid at 2, 3, 4, 6, 8, 10 and 12 Degrees

An additional analysis step was to simulate the effects of millimeter scale wrinkles using a fine mesh FEM with grids at the millimeter scale and randomly varying the orientation of each mesh. This was done for various random orientation angles of the individual meshes using a Gaussian probability. The Gaussian distribution was limited to a maximum value but also resulted in a mean over all the meshes. The two numbers that worked best to make our simulation results match the test data were a maximum deviation of around 4 degrees, which resulted in a mean deviation angle of about 2.3 degrees in the Gaussian distribution. Since the distribution is Gaussian, without a bias the wrinkles all cancel out. So for each individual element of the FEM, we also introduced a fixed bias (the direction of which varied by element) of 2 deg and additional random misalignments up to the maximum of about 4 degrees.

The results of the simulation compared to some selected test results at an incidence angle of 45 degrees can be seen in Figure 4. The “collection cone” axis shows the cone angle at which reflected light was collected by the various runs of the test on the same material. The “s” axis shows the percentage of the light collected at the various angles and thus s gets larger as cone angle increases. The original definition of s (the fraction of light that is specular) used by the 1978 testing at JPL was 10 deg (that is, any light inside a cone of 10 deg is considered specular). This definition has been retained in the current test and analysis, the test spanned and included several cone angles to better characterize s.

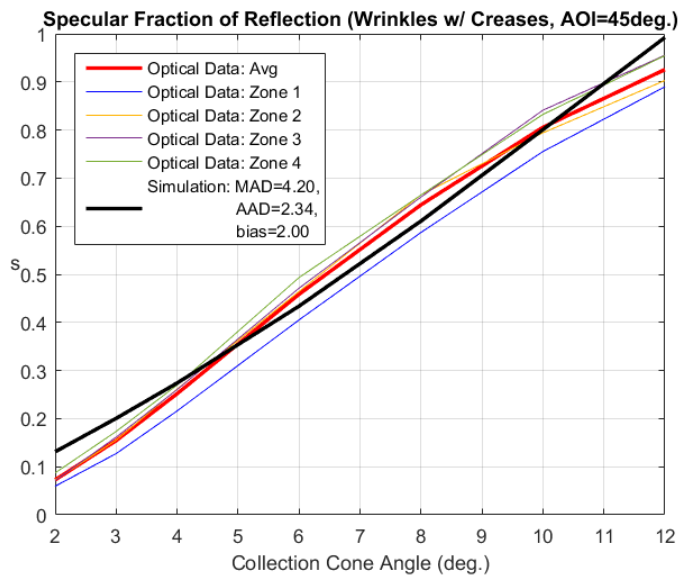


Figure 4) Simulated Mesoscale Wrinkles Compared to Test Results (Normalized for Optical Losses)

Figure 4 shows results from four regions of the sail material that correspond to four different levels of tension (labeled Zones 1 through 4). Also presented is the average of all four zones, and for comparison purposes the results of a simulated wrinkle model with a bias of 2.00 and a MAD (Maximum Angle Deviation) of 4.20 deg, which causes an AAD (Average Angle Deviation) of 2.34 deg. It can be seen in Figure 4 that the simulation does a reasonably good job of matching the test results, which demonstrates that the effect of millimeter scale wrinkles can be incorporated by modulating the value of s for the sail as a whole.

An additional note on Figure 4 is that it includes a normalization based on a test calibration. As a calibration procedure, we compared the reflected light intensity of the sail to a high reflectance Schlieren quality mirror that is

close to a perfect reflector to the intensity of the light reflected from the sail. The mirror was higher across all incidence by $\sim 20\%$. We believe the discrepancy is a combination of error due to transmission of the sail material and also error in the size of the aperture that collects light (see Figure 1). Thus the data has been normalized for optical losses (as noted in Figure 4) to account for the discrepancy between the mirror and the sail. We also calculated s by using the value of 0.91 for total reflectance. So the raw data from the test was divided by a normalization constant and the total reflectance to yield the value of s .

After eliminating test regions that were known or suspected to have errors due to test dynamics, misalignments or large wrinkles and applying the calibration normalization, we reduced the value of s from 0.94 to 0.89. However, due to the large noise and variance in the data we plan to treat 0.89 as a one-sigma variation and use the estimate of 0.80 as a 3-sigma worst-case bound for control systems studies. Note that the value of 0.80 is what actually appears in Figure 4, as Figure 4 does not include the qualitative screening described above (i.e. it includes all the noisy samples thought to be contaminated by test article dynamics and other error sources). Given the variance and noise present in the optical test data, these numbers may not be as accurate as we like, and may require more analysis, which is considered future work as resources allow.

| Coefficient | \tilde{r} | s | B_f | B_b | e_f | e_b |
|--------------------|-------------|-------------|------------|------------|-------------|-------------|
| Value | 0.91 | 0.89 | 0.79 | 0.67 | 0.025 | 0.27 |
| | ± 0.005 | ± 0.045 | ± 0.05 | ± 0.05 | ± 0.005 | ± 0.005 |

Table 3) Updated optical coefficients based on late 2015 testing

IV. Non-Flat Sail Thrust and Torque Model

Early in the NEA Scout project, we used a flat sail model for thrust and torque calculations that had a fixed Center-of-Pressure (CP) to Center-of-Mass (CM) offset of 2 cm in plane, and 2 cm out of plane. This requirement ultimately proved to be under-estimated by a wide margin. In early 2015 we discovered that the existing four quadrant sail design with booms exposed to the sun would deform severely due to thermal effects on the booms. The thermal effects were causing the ~ 7 meter long booms to deflect at the tips ~ 1 meter, which caused the solar disturbance torque to be on the order of 0.1 milli-Nm. Disturbance torques on the order of tenths of milli-Nm overwhelmed the control system by 2-3 orders of magnitude. For control and other reasons the sail model was changed to a single sail that shielded the booms from the sun. With the new single sail configuration, the disturbance torque dropped two orders of magnitude to the micro-Nm level. Although this was a great improvement, the sail was still uncontrollable with the original Attitude Control System (ACS) configuration. Thus we added an Active Mass Translator (AMT) that can shift the CM of the spacecraft in order to trim the solar torque. More details on the AMT and momentum control system for NEA Scout can be found in [Heaton]. For the purposes of this paper, we simply state that the AMT by shifting approximately 1-2 times per day over the course of the mission can reduce the solar torque to the order of tenths of nano-Nm, two orders of magnitude below the untrimmed solar torque for the single sail design. At this level of disturbance torque, the NEA Scout ACS and momentum management controller are able to achieve the mission.

In order to design the attitude and momentum control systems, a 3-dimensional solar sail disturbance torque model was required.

The nominal solar sail FEM used for the thrust and torque model is depicted in Figure 5 (note that the Z-axis is not to scale with the X and Y axes...the out of plane deformation is relatively small, but as will be seen, significant to torque). The sail FEM was obtained from Jay Warren of Langley Research Center who created an Abacus structural model that includes the effects of tension and thermal distortion. The model consists of a ~66,000 element FEM exported from Abacus that is converted into a Generalized Sail Model (GSM). The GSM consists of 39 tensor coefficients for force and 45 tensor coefficients for torque, although due to symmetries in the sail shape often not all the coefficients are unique and sometimes a small subset of those total coefficients is sufficient. The GSM thus compresses the 66,000+ elements in the FEM into a maximum of 84 coefficients contained in 6 matrices. For further information on the GSM see [Rios-Reyes multiple references].

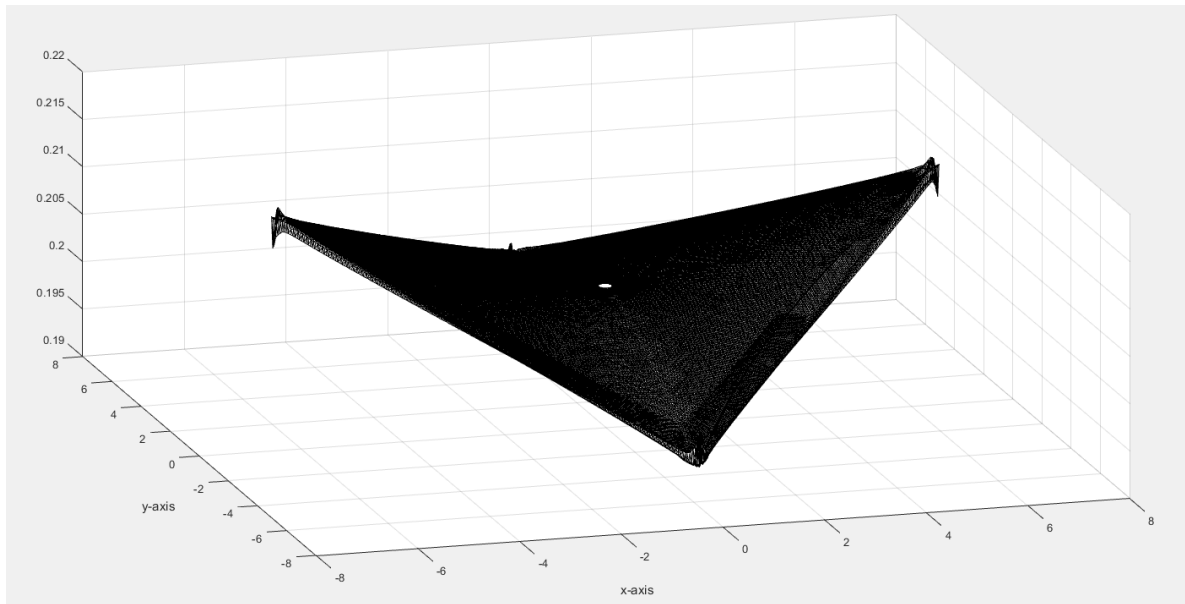


Figure 5) NEA Scout ~66,000 element FEM

The great advantage of mapping the FEM model from its original format into the GSM is the savings in computation time. As part of the momentum control system development effort, we created an optimizer to find the best position of the AMT as a function of sail attitude with respect to the sun. This optimizer needed to calculate the solar torque for all ~ 66,000 elements repeatedly for each attitude analyzed, and also to do this for all possible attitudes allowed by mission constraints (which is all attitudes at a sun incidence angle of less than 70 deg) with a certain step size (sun incidence and clock spaced 5 degrees apart). For a full optimization for a given sail model with 66,000+ elements covering all possible attitudes, the run time even on a fast computer could take anywhere from several hours to a few days. Since we needed to analyze a variety of sail models to respond to design changes and off-nominal deployments, this computational overhead was unacceptable. Mapping the FEM into the GSM reduced the run time

from on the order of a day or two to the order of a few minutes (for most sail models it takes 30-40 seconds to converge).

Figure 6 presents a comparison of thrust and torque models to a flat plate model of the same size. The results presented in Figure 6 are for the nominal sail model depicted in Figure 5. Note that the non-flat shape of the sail produces a significantly different torque, but thrust is essentially unchanged. Thus for NEA Scout, a flat plate model can suffice for thrust predictions but a realistic shape model is essential to sizing the control system properly. It can be seen in Figure 6 that the maximum torque on the non-flat sail occurs at a sun incidence angle of approximately 35 degrees, and is (as discussed above) on the order of micro-Nm.

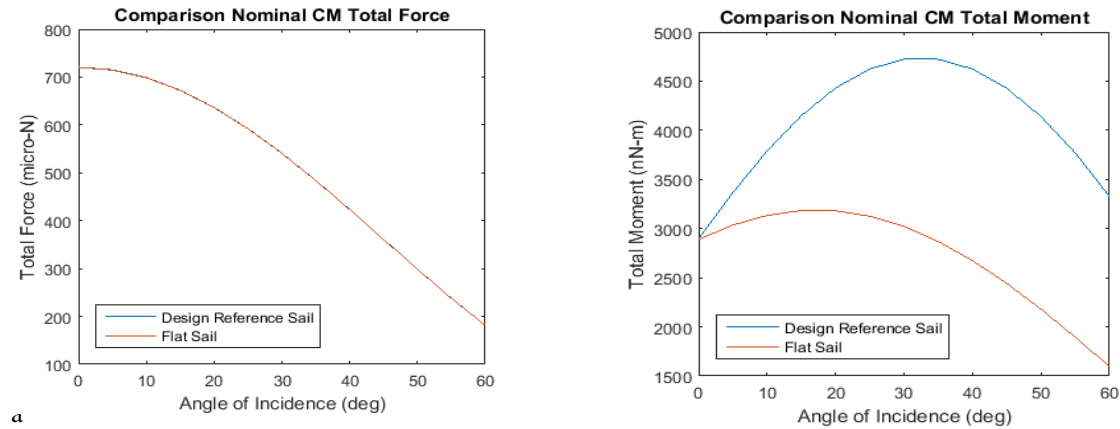


Figure 6) Nominal non-flat sail model compared to flat plate sail of equal area

That is not to say that we are sanguine that the sail model depicted in Figure 5 is an accurate prediction of the shape on orbit. It is possible or even likely that the shape will be different, perhaps significantly, and this is in fact considered one of the biggest risks to mission success. For this reason, many other off-nominal sail shapes have been considered, for design variants, different thermal conditions, and even stochastic variations on the boom tip displacements. A full discussion of these results is beyond the scope of this paper, but it is sufficient to say that off-nominal sail shape variations have been extensively considered and that the current control and momentum management systems have enough margin for torques 2-3 times as high as depicted in Figure 6 (on the order of ~ 10 micro-Nm).

V. Conclusions

We have completed an extensive review of the literature and previous optical test results and added a new test to assess the effect of wrinkles on the sail material specular fraction of reflection. We have determined that for wrinkles up the size of ~ millimeters (mesoscale wrinkles), the primary effect can be modeled as a change in the global fraction of specular reflection “s”. Since as can be seen in Equation (1)

References

- [1] Heaton, A., Orphee, J., Diedrich, B., Stiltner, B., Becker, C., "Solar Sail Attitude Control System for the NASA Near Earth Asteroid Scout Mission", *4th International Symposium on Solar Sailing*, Kyoto, Japan, Jan. 2017.
- [2] Whorton, M., Heaton, A., Pinson, R., Laue, G., Adams, C., "NanoSail-D: The First Flight Demonstration of Solar Sails for Nanosatellites", *AIAA/USU Conference on Small Satellites*, Logan, Utah, Aug. 2008, SSC08-X-1.
- [3] Ellis, J., Lisano, M., Wolff, P., Evans, J., Bladt, J., Scheeres, D., Rios-Reyes, L., and Lawrence, D., "A Solar Sail Integrated Simulation Toolkit", *Proc. AAS/AISS Spaceflight Mechanics*, Maui, HI, Feb., 2004, AAS 04-283.
- [4] Heaton, A., "GN&C Solar Sail Model Comparisons", *AIAA Guidance, Navigation and Control Conference*, Providence, Rhode Island, Aug., 2004, AIAA 2004-4890.
- [5] Vallado, D., *Fundamentals of Astrodynamics and Applications*, Springer, 2007, New York, NY Chapter 14.
- [6] Harris, M., *Spacecraft Gravitational Torques*. National Aeronautics and Space Administration. Langley, VA., 1969, NASA-SP 8024.
- [7] McInnes, C., *Solar Sailing: Technology, Dynamics and Mission Applications*, Praxis Publishing Ltd. Chichester, 1999, UK, Chapter 2.
- [8] Wertz, J. (Ed). *Spacecraft Attitude Determination and Control*. Hingham, MA, 1978, D. Reidel Publishing Company, Inc.
- [9] Nehls, M., "CP1 Environmental Effects Testing", NASA MSFC Technical Report, Sep., 2005.
- [10] Wie, B., "Dynamic Modeling and Attitude Control of Solar Sail Spacecraft", NASA Solar Sail Technology Working Group (SSTWG) Final Report Jan. 10, 2002.